Polymer Chemistry

Cite this: *Polym. Chem.*, 2012, **3**, 2277

www.rsc.org/polymers

PAPER

Electrochromic properties of a poly(dithienylfuran) derivative featuring a redox-active dithiin unit†

Sandeep Kaur,[a] Neil J. Findlay,[a] Alexander L. Kanibolotsky,[a] Saadeldin E. T. Elmasly,[a] Peter J. Skabara,*[a] Rory Berridge,[b] Claire Wilson[c] and Simon J. Coles[d]

Received 27th April 2012, Accepted 25th May 2012
DOI: 10.1039/c2py20277h

A teraryl monomer containing a 1,4-dithiin-furan central unit has been synthesised and characterised by single crystal X-ray crystallography. The di(thienyl)furan monomer **11** was successfully polymerised electrochemically and shown to possess a lower electrochemical band gap than its terthiophene analogue (1.97 eV *cf.* 2.11 eV). The electrochromic properties of this polymer proved to be superior to PEDOT, with fast switching and reversible colour transformation at high colour contrast (CE = 212 $cm^2\ C^{-1}$ *cf.* 183 $cm^2\ C^{-1}$ for PEDOT at 95% optical switch).

Introduction

Over the past four decades, organic macromolecules with extended π-conjugation have been employed in many applications such as optical displays,[1,2] solar cells,[3–5] organic field-effect transistors,[6,7] batteries[8,9] and sensors.[10] Organic electrochromic materials offer key advantages over existing inorganic materials, namely high colouration efficiency,[11] enhanced stability, faster response times, flexibility, a wider colour range and wide absorption characteristics from UV to near IR.[12–14] Electrochromic materials have the ability to undergo a reversible visible switch upon electrochemical doping. During a redox process, the applied potential breaks and rearranges π-bonds within the material, causing a change in the electronic structure of the molecule, which in turn affects the absorption characteristics of the polymer.[15,16] These smart materials have the potential to be employed in many applications, such as anti-glare mirrors in cars,[12] smart windows,[17,18] reusable labels,[19] electrochromic sunglasses,[20] adaptive camouflage,[21,22] near-IR telecommunication[23] and displays.[18,24]

Electrochromic devices can be fabricated from a range of materials, but conjugated polymers excel in the properties outlined above.[2,18,25] These simple organic molecules can provide exceptional materials for the fabrication of full-colour electrochromic devices[1,10,26] using various processes.[27,28] The optical and physical properties of organic materials can be fine-tuned through structural modification, such as, the introduction of various substituents; alkyl-chain side groups aid solubility, whilst the presence of electron-withdrawing or donating groups can alter the band gap.[29,30] Polyheterocyclic polymers such as polypyrrole,[23] polythiophene,[31,32] polyselenophene[33–35] and their derivatives have been extensively studied since they possess chemical and electrical stability in both neutral and doped states.[25] The electrical and optical properties of these polymers are highly influenced by the change in electronegativity of the heteroatom.[36]

Polyfurans have not been intensively investigated as an electrochromic material, despite possessing many similar characteristics to thiophene.[37–40] These furan derivatives are naturally occurring materials and are readily biodegradable.[41,42] Unfortunately, furans are known to have a high oxidation potential (*ca.* 2 V), but with band gap engineering *via* the introduction of electron-rich systems or extension of conjugation, this problem can be overcome.[43,44]

Bendikov *et al.* have shown oligofurans to have increased fluorescence, a higher HOMO, better packing, greater rigidity and efficient processability compared to their thiophene analogues.[38,45,46] These oligofurans can be used as p-type semiconductors in OFETs, showing similar field effect mobilities to the thiophene analogue,[47] leading to the development of new 'green' organic semiconductors.[48] Fréchet *et al.* have been pursuing this idea and recently revealed a bulk heterojunction solar cell fabricated from furan-containing polymers and $PC_{71}BM$ with a power conversion efficiency of 5%.[42] The incorporation of furan units into a conjugated backbone has been shown to enhance the solubility of mixed thiophene–furan oligomers compared to the all-thiophene analogues.[49] Additionally, the morphological properties of the polymer would differ due to the presence of the smaller, more electronegative oxygen atom in place of the larger sulfur atom.[43]

[a]*WestCHEM, Department of Pure and Applied Chemistry, University of Strathclyde, Glasgow G1 1XL, UK. E-mail: peter.skabara@strath.ac.uk; Fax: +44 (0)141 548 4822; Tel: +44 (0)141 548 4648*
[b]*DSTL, Physical Sciences Department, Porton Down, Salisbury, Wiltshire SP4 OJQ, UK*
[c]*National Crystallography Service, Diamond Light Source Ltd, Diamond House, Harwell Science & Innovation Campus, Didcot, Oxfordshire, OX11 ODE, UK*
[d]*National Crystallography Service, School of Chemistry, University of Southampton, Highfield, Southampton, SO17 1BJ, UK*
† CCDC [879413]. For crystallographic data in CIF or other electronic format see DOI: 10.1039/c2py20277h

Recently, we reported two polymers, **Poly1** [50] and **Poly2**,[51] which were structurally designed as electrochromic materials (see Fig. 1). **Poly1** bears a quinoxaline heterocycle fused to the central thiophene ring of the repeat unit *via* a 1,4-dithiin bridge. This polymer was found to have superior switching speeds than poly(3,4-ethylenedioxythiophene) (PEDOT) (ΔT 44% optical change in 1 s, *cf.* 2.2 s for PEDOT). The fast switching response of **Poly1** is a result of the non-planar nature of the repeat units, facilitated by the boat conformation of the non-aromatic dithiin rings.[51] This suggests that the loosely packed polymer allows efficient ingression/egression of ions throughout the film during chemical redox processes and hence improves switching speeds. It is anticipated that the marriage of furan and a dithiin ring within a conjugated polymer would provide interesting chemical and physical properties compared to the all-thiophene analogue.[51] This report describes a general synthetic route to three novel furan monomer units, **7**, **8** and **11**, together with the successful electropolymerisation of monomer **11** to form **Poly3**. This polymer is studied further as an electrochromic material.

Results and discussion

Synthesis

Monomers **7**, **8** and **11** were prepared according to Scheme 1. Initially, cycloaddition of alkyne **1** [52] with 1,3-dithiole-2,4,5-trithione oligomer (DMIT) **2**,[53] using a literature-based method,[54] was followed by reduction of the resulting aldehyde **3** to give alcohol **4**. The acid-catalysed cyclisation[55] of the alcohol **4** gave the furan derivative **5** in an 87% yield. Thione **5** was further transchalcogenated into the corresponding carbonyl derivative **6** in high yield, which was subsequently converted to the dithiolate and alkylated to give bis(methylthio)dithiino furan **7** or bis(hexylthio)dithiino furan **8**. Compound **7** was further functionalised by bromination with *N*-bromosuccinimide and subsequently used for Stille cross-coupling with stannylated thiophene **10** to afford monomer **11** in 22% yield.

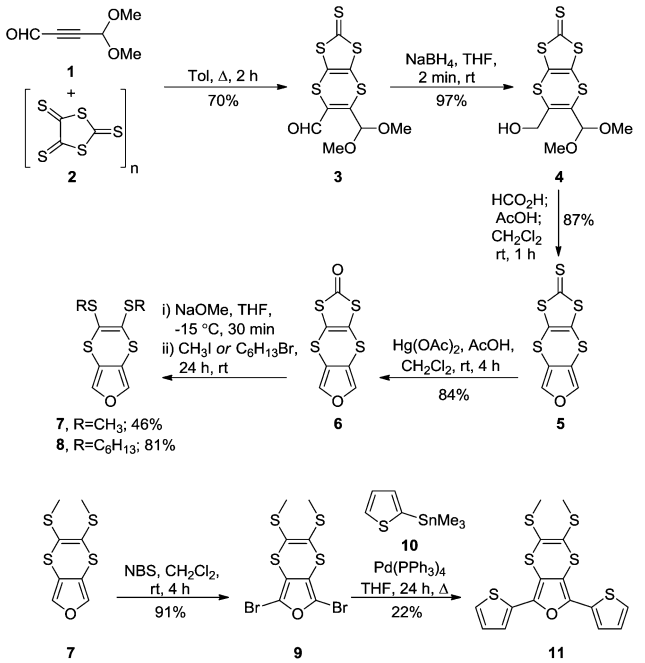

Scheme 1 Synthetic route to furan-containing monomers **7**, **8** and **11**.

Absorption spectroscopy and electrochemistry of monomers

The electronic absorption spectra for the three monomers were recorded in dichloromethane solution (see Table 1). As expected, the absorption maxima for monomers **7** and **8** are similar given their near identical structures (268 and 267 nm, respectively). However, as anticipated the increase in conjugation length to a teraryl unit in monomer **11** leads to a π–π^* transition at 342 nm.

In cyclic voltammetry (CV) experiments, the structurally similar monomers **7** and **8** showed one quasi-reversible, anodic oxidation peak at +0.55 and +0.65 V and a second irreversible anodic oxidation peak at +0.91 and +0.98 V, respectively (see Fig. 2 and Table 1). The CV of di(thienyl)furan monomer **11** revealed two anodic oxidation processes at +0.76 and +1.11 V with the latter being irreversible. The electrochemical HOMO–LUMO gaps of the monomers were calculated from the difference in the onset of the first oxidation and reduction peaks. The increase in the electrochemical HOMO–LUMO gap of monomer **11** is unexpected in comparison to monomer **7** and **8** (2.98 V compared to 2.42 V and 2.37 V respectively). All three monomers retain similar HOMO levels whilst monomer **11** shows the LUMO level to have moved towards vacuum. This rise in LUMO of monomer **11** can be rationalised by the inductive effect of the thiophene ring pushing electron density towards the central furan core and thus making monomer **11** a poor electron acceptor. The spectral and electrochemical properties of all three monomers clearly reveal significant differences when comparing their optical and electrochemical HOMO–LUMO gaps. It can be hypothesised that the 1,4-dithiin ring side group shows some reductive electroactivity that is independent from the heterocyclic core.[50]

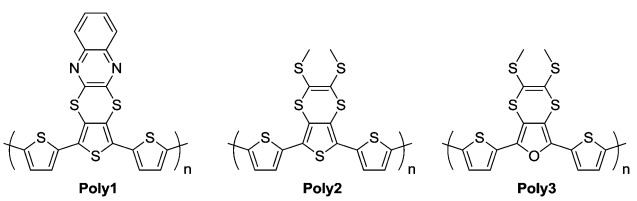

Fig. 1 Structures of **Poly1**, **Poly2** and **Poly3**.

Electropolymerisation

Electrochemical oxidative polymerisation of monomers **7** and **8** was unsuccessful despite continuously cycling over both redox peaks and this is explained later. However, monomer **11** polymerised readily onto a carbon-working electrode during repetitive cycling over the first oxidation peak. The growth trace is displayed in Fig. 3. Once **Poly3** was deposited on the carbon-working electrode, it was dedoped to neutral by repetitive cycling in a region of no electroactivity (−0.4 to +0.1 V), before its electrochemistry was investigated in monomer-free acetonitrile solution (see Fig. 4). When a polymeric species is formed the conjugation length is increased, giving rise to a new lower

Table 1 HOMO and LUMO values are calculated from the onset of the first peak of the corresponding redox wave and referenced to ferrocene, which has a HOMO of −4.8 eV. Electronic absorption spectra all recorded in CH_2Cl_2

Monomer	E_{ox1}[a]/E_{ox1}[b] (V)	E_{ox2} (V)	E_{red} (V)	HOMO (eV)	LUMO (eV)	HOMO − LUMO (eV)	UV-Vis λ_{max} (nm)	Optical gap (eV)
7	0.55[c]/0.48	0.91[d]	−2.07	−5.34	−2.92	2.42	268	—
8	0.65[c]/0.57	0.98[d]	−2.08	−5.28	−2.91	2.37	267	—
11	0.76[c]/0.67	1.11[d]	−2.36	−5.43	−2.45	2.98	342	3.07

[a] Anodic peak. [b] Cathodic peak. [c] Quasi-reversible peak. [d] Irreversible peak.

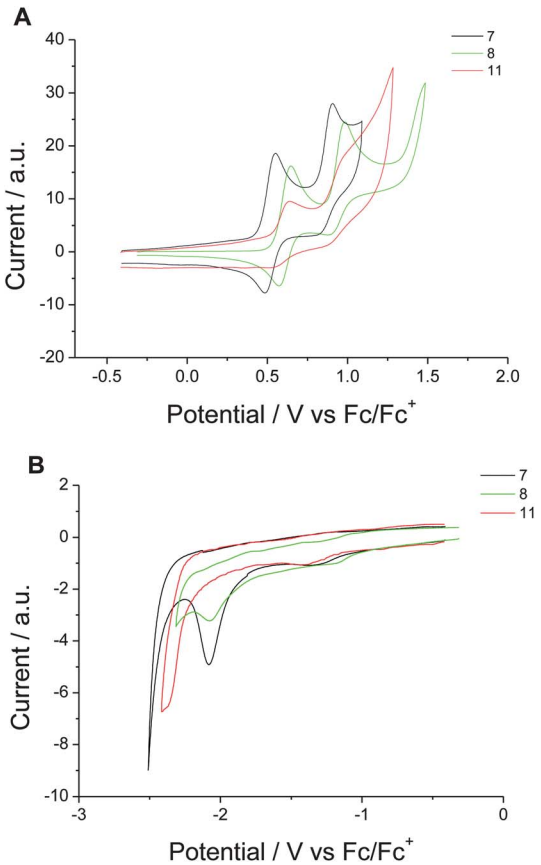

Fig. 2 Cyclic voltammograms: (A) oxidations and (B) reductions of monomers **7**, **8**, **11** in CH_2Cl_2 solution (glassy carbon working electrode, silver wire pseudoreference, $TBAPF_6$ as the supporting electrolyte (0.1 M), substrate concentration 10^{-4} M, scan rate 100 mV s^{-1}). The data was referenced to the Fc/Fc^+ redox couple.

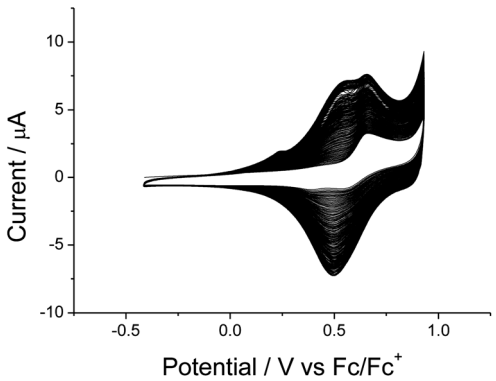

Fig. 3 Electrochemical growth of monomer **11** using a glassy carbon working electrode, Ag wire pseudo-reference electrode, platinum counter electrode, $TBAPF_6$ as supporting electrolyte (0.1 M), substrate concentration 10^{-4} M, oxidative voltage sweep ran from 0 to 1 V over 150 cycles. The scan rate was 100 mV s^{-1}.

oxidation peak. The oxidation of **Poly3** exhibits a large broad reversible wave at +0.63 V, compared to the all-thiophene analogues **Poly1** [50] at +0.40 V and **Poly2** [51] at +0.60 V. This broad redox wave could be due to the simultaneous oxidation of the 1,4-dithiin and bithiophene units, which are both electroactive. UV-Vis absorption of **Poly3** revealed a significant bathochromic shift compared to monomer **11** (474 nm for **Poly3** *cf.* 342 nm for monomer **11**, see Fig. 4), a result of the increased effective conjugation length. The onset of the absorption edge for the longest wavelength band is at 650 nm, giving an optical band gap of 1.90 eV. This value corresponds closely to the electrochemical band gap of **Poly3** obtained by cyclic voltammetry (1.97 eV, see Table 2).

Interestingly, we have shown the furan-based **Poly3** to have both a lower electrochemical and optical band gap when compared to its thiophene analogue **Poly2** (see Table 2). Recent reports by Bunz have demonstrated bithiophene rings to twist by 22.6° with respect to one another, whilst bifuran monomers were found to be planar.[38] Their study pointed to steric hindrance between the larger sulfur atom and the 3′-hydrogen of the adjacent ring, which was not evident in bifuran due to the smaller oxygen atoms.[38] Additionally, the difference in electronegativity and less aromatic character of the furan ring *cf.* thiophene contributes to the narrower band gap of **Poly3**.

X-ray crystallography

The structure of monomer **11** was determined by single crystal X-ray diffraction. In general, dithiin rings are known to adopt a boat conformation, with the degree of bending in the ring expressed as a folding along the S···S vector (see Fig. 5); the hinge angle along the S···S vector is 137° and 133° for the two independent molecules. Monomer **11** retains a high degree of planarity between the adjacent thiophene units bound to the furan core. Two molecular conformers are present within the unit cell – one conformer shows both peripheral thiophene units to be *anti* to the furan (torsion angles O1–C1–C9–S2 169(2)°, O1–C4–C5–S1 176(2)°), forming close S···S intramolecular contacts with the 1,4-dithiin ring on the furan (S2···S4 3.43, S1···S3 3.33 Å). The other conformer within the unit cell exists with one peripheral thiophene unit in the *anti* conformation with respect to the furan (O1a–C4a–C5a–S11a = −176(2)°,

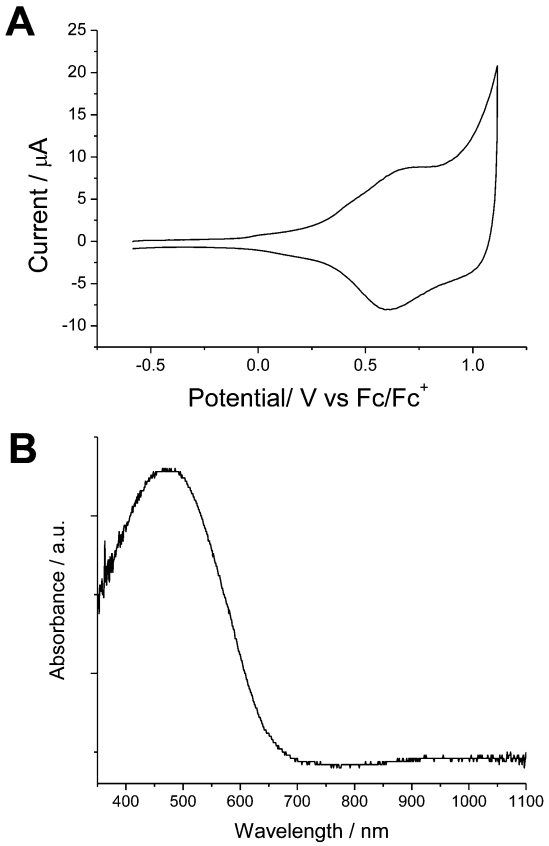

Fig. 4 (A) Oxidation of **Poly3** film after dedoping of polymer in MeCN solution. The data is referenced to the Fc/Fc^{+} redox couple. The E_g gap was calculated from the onset of the first peak of the corresponding redox wave (reduction process not shown here) and referenced to ferrocene, which has a HOMO of −4.8 eV. (B) Electronic absorption spectrum of **Poly3** deposited as a thin film on ITO glass.

S11a···S3a = 3.39 Å) and the other to be either in the *anti* or *cis* conformation in a 1 : 1 ratio (O1a–C1a–C9a–S2a = 173(2)°, O1a–C1a–C9a–S2a = −7(3)°, S2a···S4a = 3.35 Å for the *anti* conformation). There is some sign of disorder between the *cis* and *trans* conformation for the other thiophene rings but to a much lesser degree and it was not modelled.

Theoretical calculations

The unsuccessful electropolymerisation of monomers **7** and **8** can be explained *via* molecular modelling calculations. Computational calculations were performed using density functional theory (DFT) at the B3LYP/6-31G* level (Spartan'10) on monomer **7**. The HOMO is situated predominantly over the dithiin ring, with a small contribution on the furan ring (Fig. 6). The 1,4-dithiin ring is a better electron donor than the furan fragment and is most likely to donate the first electron upon oxidation. The LUMO resides across the four sulfur atoms and two sp^2 carbons between the heteroatoms. Examination of the SOMO (the radical cation of monomer **7**) reveals that electron spin density is localised within the dithiin ring. To initiate successful radical polymerisation of monomer **7** the system requires electron spin density on either the 2- or 5-position of the furan ring. Thus, it would appear that successful electropolymerisation of monomer **7** (or **8**) does not occur at potentials below that which would cause monomer decomposition (>2 V).

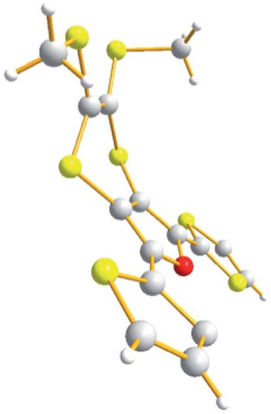

Fig. 5 View showing the crystal structure of one of the two independent molecules of monomer **11**, viewed along the *a*-axis.

Spectroelectrochemistry

The UV-Vis spectroelectrochemical measurements of the neutral **Poly3** film deposited on an ITO glass substrate were investigated in monomer-free acetonitrile solution with the same electrolyte concentration as before (see Fig. 7). Spectroelectrochemical studies improve our understanding of transient chemical species generated *in situ* during redox reactions occurring at the electrode surface.[56,57] The spectroelectrochemical plot shows the generation of new absorption waves forming at +0.9 V in the wavelength region of 600–1100 nm alongside the concomitant loss of intensity of the π–π* band at 474 nm. The optical transition observed at *ca.* 600 nm is evidence of the formation of positively delocalised polaron species within the polymer chain and, upon further oxidation, a broader optical transition near 900–1100 nm represents the

Table 2 Electrochemical and absorption spectroscopy data for thin films of **Poly3** compared to the analogous polymer **Poly2** and **Poly1**

Polymer	E_{ox1} (V)	E_{ox2} (V)	E_{red} (V)	HOMO (eV)	LUMO (eV)	E_g (eV)	UV-Vis λ_{max} (nm)	Optical gap (eV)
Poly1[50]	+0.40	1.20	−1.87	—	—	1.85	467	1.90
Poly2[51]	+0.60	0.83	−1.93	−5.30	−3.19	2.11	450	2.00
Poly3	+0.63[a]/+0.22[b]	—	−2.14	−5.02	−3.05	1.97	474	1.90

[a] Broad quasi-reversible anodic peak. [b] Peak onset.

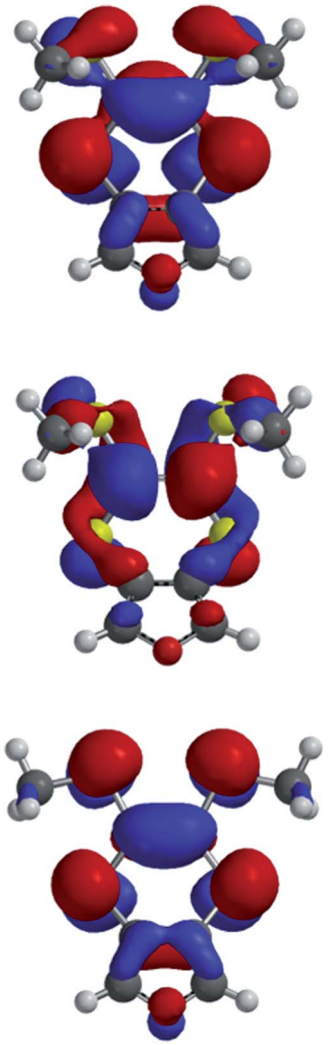

Fig. 6 Top: HOMO, middle: LUMO and bottom: SOMO plots of monomer **7**.

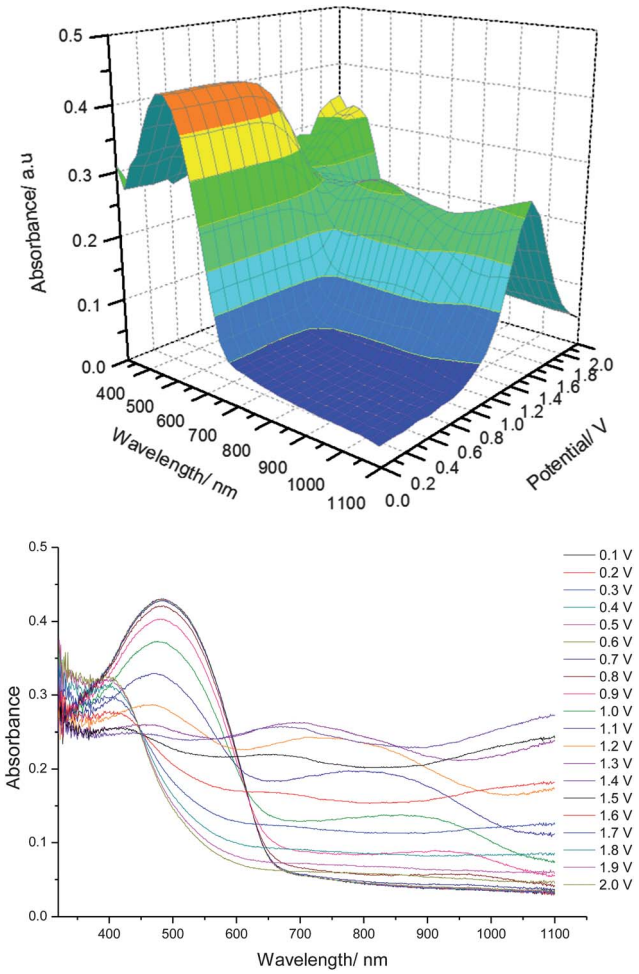

Fig. 7 Top: 3D absorption spectroelectrochemical plot; bottom: 2D absorption spectroelectrochemical plot of oxidation of **Poly3** in acetonitrile solvent.

propagation of doubly charged bipolaron species.[56] These spinless bipolaron species are thermodynamically stable when structurally manipulating the polymer chain from its aromatic structure and adopting the quinoidal polymer form.[56,58] The bond length between neighbouring heterocycles is contracted when in the quinoidal form, which allows efficient orbital overlap and charge delocalisation.[56,57] Additionally, the 1,4-dithiin pendant groups of the conjugated polymer oxidise at lower potentials as illustrated in cyclic voltammograms for monomers **7**, **8**, **11** and **Poly3** (see Fig. 2 and Fig. 4). However, the oxidised 1,4-dithiin rings are not spectroscopically detected due to the weak sulfur n–π* transitions. Fig. 7 (bottom), illustrates the spectro-electrochemical studies of **Poly3** in a 2D plot and clearly shows the formation of polarons and bipolarons upon increasing potentials. At higher oxidation potentials (>1.4 V) the spectral profile differs and shows the formation of a new absorption wave at *ca.* 400 nm. This signifies the polymer morphology has changed and is possibly due to an over population of the bipolaron species, which increases the polymers electrophilicity and susceptibility to nucleophilic attack by water molecules/OH^- ions or other nucleophilic impurities that may be present in the investigating medium.[58,59] Thus, it would result in non-reversible formation of the polymer with shorter conjugation lengths. To overcome such issues, polymer films can be encapsulated into devices or supported with a gel electrolyte coating.[57,60] Spectroelectrochemical studies have clearly illustrated **Poly3** undergoing reversible redox changes at oxidation potentials lower than 1.4 V with different optical responses from visible to the NIR region.

Switching studies

The switching ability of **Poly3** was studied by measuring the wavelength at which the greatest absorbance change is experienced when stimulated between two different potentials. The potential switch from 0 to +1.3 V causes a change in the polymeric state from neutral to p-doped. The rate of change in transmittance upon oxidation/reduction provides a direct indication of the switching ability of a material, an important property for display industries. **Poly3** was grown on ITO glass and dedoped. The transmittance was monitored at 705 nm as the potential was switched between 0 and +1.3 V (*vs.* Ag wire) using

square wave potentiometry, as shown in Fig. 8. The switching characteristics of the polymer were followed over cycles of 10, 5, 2.5, 1.25, 0.5, 0.25 s and the change in transmittance was 83.9, 79.8, 72.9, 62.4, 39.8 and 23.8%, respectively. One reason for this fast optical change is the bent 1,4-dithiin ring conformation, a feature of both **Poly2** and **Poly3**, which distorts the π–π stacking and creates an open morphology, thus allowing the efficient flow of counterions into and out of the polymer film.[51] However, **Poly3** shows a faster and greater change compared to the analogous terthiophene **Poly2** (see Table 3). The single difference being that **Poly3** contains one furan to every two thiophene units. It is not clear why, but the subtle incorporation of an oxygen atom, providing a less aromatic furan ring, improves the switching properties compared to the all thiophene analogue.

Colorimetry

The CIE colour coordinates of **Poly3** electrochemically deposited on ITO were measured in monomer-free acetonitrile solution with the same electrolyte concentration as previously stated. The analysis is reported *via* the 1931 (*Yxy*) CIE and 1964 ($L^*a^*b^*$) CIE representation of colour space as recommended by the "Commission Internationale de L'Eclairage" (CIE).[61] The

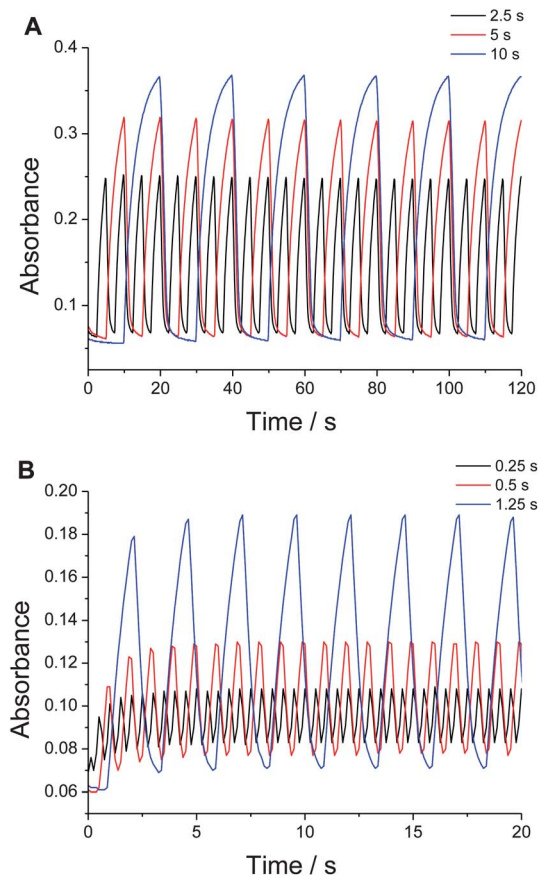

Fig. 8 Both graphs (A) and (B) show change in absorbance upon p-doping at various switching rates for **Poly3** in acetonitrile solution. Absorbance was monitored at 705 nm between potentials of 0 and +1.3 V.

Table 3 Switching times and percentage change in absorbance

	Time (s)					
	10	5	2.5	1.25	0.5	0.25
Δ*T*% **Poly3**	83.9	79.8	72.9	62.4	39.8	23.8
Δ*T*% **Poly2**[a]	79.8	66.2	51.6	39.3	19.0	9.3

[a] Absorbance was measured at 755 nm between potentials of −0.4 and 1.5 V of **Poly2** in acetonitrile solution.[51]

measurements recorded were using a 10° standard observer and Source C illuminant (overcast daylight, CIE 1964, 6770 K). *Y* is defined as the luminance of the CIE *XYZ tristimulus* values, which are assigned to the red, green and blue curves respectively.[62] The L^* coordinates represent the brightness of the material ranging from 0–100. A positive a^* value represents the redness; whilst the negative a^* value represents the greenness of the sample.[63] Complementary, a positive b^* is yellow and a negative b^* is blue in colour. The polymer film was subjected to constant applied potential at 0 V then +1.3 V for a duration of 90 seconds to achieve the neutral and doped state, whilst the colour coordinates were measured to determine the colour transformation, see Table 4.

The optical change experienced can be seen by the naked eye. **Poly3** shows a reversible transition from salmon-red to a beige tan colour (see inset in Fig. 9), whilst the closely related polymer **Poly2** shows an optical change from red to yellow.[51]

Colouration efficiency (chronocoulometry)

Colouration efficiency (CE) is a parameter, which characterises the ability of the material to change absorbance upon injecting electric charge during oxidation (or reduction). CE is expressed as:[64]

$$\eta = \Delta\mathrm{OD}(\lambda)/Q_\mathrm{d} \quad (1)$$

$$\Delta\mathrm{OD} = \log[\%T_\mathrm{b}(\lambda)/\%T_\mathrm{c}(\lambda)] \quad (2)$$

The optical density at a specific wavelength (λ_{max}) was determined by using %*T* values of bleached ($\%T_b$) and coloured films ($\%T_c$) using eqn (2). The colouration efficiency (η) of the material can be calculated by using eqn (1), where $\Delta\mathrm{OD}(\lambda)$ is the change in optical absorbance, and Q_d is the charge density which causes $\Delta\mathrm{OD}(\lambda)$.[64]

Chronocoulometry studies were performed on neutral state **Poly3**, electrochemically deposited onto an ITO slide in monomer-free acetonitrile solution. This film was subjected to a low current through the film, leading to a colour transformation over a 30 second interval.[65,66] Fig. 9 shows the simultaneous measuring of % change in transmittance of the film, and charge flow during a complete switch. The electrochromic film was monitored at $\lambda_{max} = 705$ nm as the voltage was pulsed for a 10 second step between the neutral state (0 V) and the oxidised state (+1.3 V), see Fig. 9.

According to eqn (1) and (2), the CE of **Poly3** was calculated to be 212 $cm^2\ C^{-1}$ at 95% of full switch ($\lambda_{max} = 705$ nm), which is higher than that of closely packed PEDOT film (183 $cm^2\ C^{-1}$),

Table 4 CIE *Yxy* 1931 and *L*a*b** 1964 colour space for **Poly3** in the neutral and doped form using 10° standard observer and Source C illuminant

	X	*Y*	*Z*	*x*	*y*	*z*	*L**	*a**	*b**
Poly3 neutral	55.45	50.56	45.48	0.3660	0.3338	0.3002	76.41	16.21	13.01
Poly3 doped	55.78	57.50	54.84	0.3318	0.3420	0.3262	80.46	−0.42	10.57

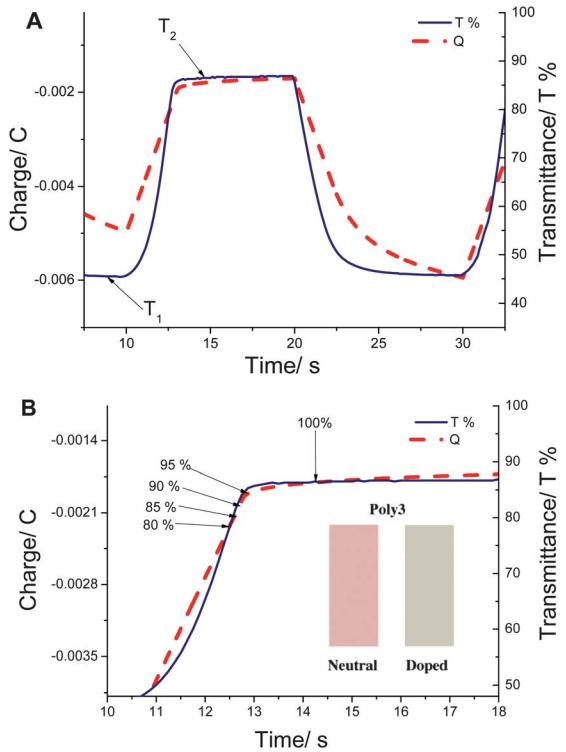

Fig. 9 (A): colouration efficiencies (chronocoulometry) experiments of **Poly3** film on ITO, switched from fully neutral (0 V) to fully oxidised state (+1.3 V) and back to neutral state, 3 steps for 10 second pulse and transmittance measured at $\lambda_{max} = 705$ nm. (B) graph shows various % optical changes from which to calculate CEs. Inset: Adobe Photoshop images to represent **Poly3**'s colour switch, images created by conversion of CIE *Lab* to CIE *XYZ* coordinates.

but slightly lower than that of PProDOT (285 cm^2 C^{-1}),[67] see Fig. 9 and Table 5. Comparatively, **Poly1** (possessing large quinoxaline pendant groups) shows superior CE of 381 cm^2 C^{-1} measured at 650 nm for a 95% full switch.[50] Colouration efficiency studies highlight how subtle structural modification in organic polymers can influence electrochromism performance.[67]

Conclusions

Three new furan-based monomers were synthesised and characterised by absorption spectroscopy and cyclic voltammetry. Monomer **11** was successfully electropolymerised to form **Poly3** and investigated by UV-Vis spectroelectrochemistry and electrochromic switching studies. **Poly3** exhibited a lower electrochemical band gap of 1.97 eV and superior switching speeds than its corresponding terthiophene analogue.[51] This is explained by the lower aromaticity of furan systems over thiophene analogues with **Poly3** possessing efficient charge delocalisation across the polymer backbone than the previously published analogues.[38] **Poly3** showed a reversible optical transformation from a red salmon colour when neutral, to a beige tan colour in the doped form, with a higher colour contrast than PEDOT[67] (212 cm^2 C^{-1} *cf.* 183 cm^2 C^{-1} at 95% full switch). The incorporation of a furan unit has improved the electrochromic properties compared to its all-thiophene analogue.[51]

Experimental

General

^{1}H and ^{13}C NMR spectra were recorded on a Bruker Avance AV3 400 or DRX 500 apparatus at either 500.13 and 125.76 MHz or 400.13 and 100.61 MHz, in $CDCl_3$. Chemical shifts are given in ppm; all *J* values are in Hz. Elemental analyses were obtained on a Perkin-Elmer 2400 analyzer. Electron absorption spectra were measured on a Unicam UV 300 spectrophotometer. MS LDI-TOF spectra were run on a Shimadzu Axima-CFR spectrometer (mass range 1–150 000 Da). IR spectra were recorded an ATR Microlab PAL spectrometer. Melting points were taken using a Stuart Scientific SMP1 Melting Point apparatus and are uncorrected. Column chromatography was performed with commercially available solvents and using VWR silica gel (40–63 μm). Thin layer chromatography (TLC) was performed using aluminium plates precoated with Merck silica gel 60 (F_{254}) and visualised by ultra-violet radiation and/or iodine vapor. All reagents were purchased from Sigma-Aldrich or Alfa Aesar and were used without further purification, unless stated otherwise. Anhydrous solvents were obtained from a PureSolv solvent purification system.

Table 5 Colouration efficiencies determined for **Poly3** at various % optical changes of complete colour switch

$\Delta T^{a,b}$ (%)	% Change	$T_c{}^a$ (%)	$T_b{}^a$ (%)	τ (s)	*Q* (C)	$Q_d{}^c$ (C cm^{-2})	ΔOD^d	η^e (cm^2 C^{-1})
40.91	100	45.51	86.42	5.36	3.02×10^{-3}	1.34×10^{-3}	0.279	207.45
38.86	95	45.51	84.37	3.86	2.84×10^{-3}	1.26×10^{-3}	0.268	212.39
36.82	90	45.51	82.33	3.76	2.74×10^{-3}	1.12×10^{-3}	0.257	211.41
34.77	85	45.51	80.28	3.68	2.66×10^{-3}	1.18×10^{-3}	0.247	208.51
32.73	80	45.51	78.24	3.61	2.60×10^{-3}	1.16×10^{-3}	0.235	203.64

[a] Transmittance measured at $\lambda_{max} = 705$ nm. [b] $\Delta T\% = T_b\% - T_c\%$ [c] $Q_d = Q/A$, where *A* (Electrode area) = 2.25 cm^2 [d] $\Delta OD = \log[\%T_b/\%T_c]$ [e] $\eta = \Delta OD(\lambda)/Q_d$.

X-ray crystallography

Data for **11** were collected on an Enraf Nonius Kappa CCD using Mo-Kα radiation, as ϕ scans and ω scans to fill the Ewald sphere. Data collection, cell refinement and data reduction were carried out using COLLECT[68] and DENZO.[69] The structure solution was obtained by direct methods (SHELXS-97)[70] and a full-matrix least-squares refinement on F^2 was performed on all reflections by SHELXL-97 [70] in the OLEX2 environment.[71]

Crystal structure determination of monomer 11

Crystal data. $C_{16}H_{12}OS_6$, $M = 412.61$, monoclinic, $a = 22.338(3)$, $b = 4.7901(7)°$, $c = 17.757(3)$Å, $\beta = 113.326(7)°$, $U = 1744.7(4)$Å^3, $T = 120$ K, space group Pc (no. 7), $Z = 4$, 11 738 reflections measured, 5748 unique ($R_{int} = 0.142$) which were used in all calculations. The final $wR(F^2)$ was 0.265, $R_1 = 0.12$ for 3919 observed data. The CCDC deposition number is: 879413.

Electrochemistry

CV measurements were performed on a CH Instruments 660A electrochemical workstation with *iR* compensation using anhydrous dichloromethane or acetonitrile as the solvent. The electrodes were glassy carbon, platinum wire, and silver wire. All solutions were degassed (Ar) and contained monomer substrates in concentrations of *ca.* 10^{-4} M, together with $TBAPF_6$ (0.1 M) as the supporting electrolyte. All measurements are referenced against the $E^{1/2}$ of the Fc/Fc^+ redox couple. Spectroelectrochemical, switching and colouration efficiency experiments were conducted on ITO glass. Absorption and CIE coordinates were recorded on a UNICAM UV 300 instrument.

Synthesis

Compounds **5** and **6** were prepared using the procedure of Berridge *et al.*[72]

6-(Dimethoxymethyl)-2-thioxo-[1,3]dithiolo[4,5-*b*][1,4] dithiine-5-carbaldehyde (3)

To a solution of 4,4-dimethoxybut-2-ynal **1** (4.30 g, 0.034 mol, 3.50 ml) in 500 ml of dry toluene, oligo trithioxo-1,3-dithiole (DMIT) **2** (6.50 g, 0.50 mol) was added and this mixture was refluxed for 2 h. The solvent was removed under reduced pressure and the crude product was purified by column chromatography using toluene as eluent to give a red-orange solid **3** (7.64 g, 70%); ^{1}H NMR (400 MHz, $CDCl_3$): δ_H 3.46 (6H, s, 2 × CH_3), 5.58 (1H, s, $CHO(CH_3)_2$), 10.02 (1H, s, CHO); ^{13}C NMR (100 MHz): δ_C 53.8, 99.8, 126.9, 128.5, 134.1, 154.7, 181.7 ppm; MS: *m*/*z* GC/CI: 324.01 Da; EA_{Calc}: C, (33.31%); H, (2.49%); S, (49.41%); EA_{Found}: C, (33.19%); H (2.31%); S (49.30%). ν_{max} ATR-IR/cm^{-1}: 2958, 2833, 1669, 1552, 1496 and 1069; Mpt: 128–130 °C.

5-(Dimethoxymethyl)-6-(hydroxymethyl)-[1,3]dithiolo[4,5-*b*][1,4]dithiine-2-thione (4)

Sodium borohydride (2.94 g, 0.074 mol) was added to a stirred solution of aldehyde **3** (3.00 g, 9.25 mmol dissolved in 100 ml of THF) at room temperature. After 2 min, the reaction mixture was poured into 100 ml of saturated aqueous $NaHCO_3$, KBr (19.5 g) was added and the product was extracted with ethyl acetate (3 × 100 ml). The extract was dried over $MgSO_4$ and evaporated *in vacuo* to dryness affording the product **4** as a brown/yellow oil (2.94 g, 97%), which was used in the next step without further purification; ^{1}H NMR (400 MHz, $CDCl_3$): δ_H 2.11 (1H, s, OH), 3.39 (6H, s, 2 × CH_3), 4.48 (2H, s, H_2C), 5.24 (1H, s, CH); MS: MALDI-TOF, matrix used THAP: 345 Da and 295 Da.

2,3-Bis(methylthio)-[1,4]dithiino[2,3-*c*]furan (7)

To a cold (−15 °C) mixture of carbonyl derivative **6** (0.333 g, 1.36 mmol) in THF (20 ml) was added sodium methoxide (25%, 4.37 M, 0.22 ml) dropwise. The mixture was stirred for 30 min whilst under nitrogen. Then iodomethane (0.70 ml, 10.8 mmol) was added dropwise and the mixture allowed to reach room temperature and left to stir overnight. The solvent was removed under reduced pressure, and the residue was dissolved in chloroform, filtered and, after removal of the solvent, the crude product was subjected to column chromatography on silica gel using 20% dichloromethane in hexane as eluent. The product was isolated as a yellow crystalline solid (0.245 g, 46%); ^{1}H NMR (400 MHz, $CDCl_3$): δ_H 2.46 (6H, s, $S(CH_3)_2$), 7.26 (2H, s, (Ar-H)); ^{13}C NMR (125 MHz): δ_C 18.4, 119.2, 128.8, 137.2 ppm. MS: *m*/*z* GC/CI: 248.9 Da; EA_{Calc}: C, (38.68%); H, (3.25%); S, (51.63%); EA_{Found}: C, (39.06%); H (3.23%); S (51.15%); ν_{max} ATR-IR/cm^{-1}: 3120, 2922, 1537, 1410, 1032, 873 and 842; Mpt: 67–69 °C.

2,3-Bis(hexylthio)-[1,4]dithiino[2,3-*c*]furan (8)

To a cold (−15 °C) mixture of carbonyl derivative **6** (0.140 g, 53.4 mmol) in dry THF (30 ml) was added sodium methoxide (25%, 4.37 M, 0.52 ml) dropwise. The mixture was stirred for 30 min whilst under constant flow of nitrogen gas. 1-Bromohexane (0.62 ml, 3.2 mmol) was added drop wise and the mixture was allowed to reach room temperature and stirred overnight. The solvent was removed under reduced pressure, and the residue was treated with chloroform, filtered and after removal of solvent, the crude product was subjected to column chromatography on silica gel using 1 : 1 dichloromethane : hexane as eluent. The product was isolated as a yellow oil (0.167 g, 81%); ^{1}H NMR (400 MHz, $CDCl_3$): δ_H 0.87 (6H, t, $J = 6.6$ Hz, 2 × CH_3), 1.26 (8H, m, $-CH_2CH_2$), 1.38 (4H, quintet, $J = 7.4$ Hz $-CH_2(CH_2)_2$), 1.56 (4H, quintet, $J = 7.4$ Hz, $(-CH_2(CH_2)_3Me)_2$), 2.92 (4H, t, $J = 7.3$ Hz, $(SCH_2(CH_2)_4Me)_2$), 7.25 (2H, s, Ar-H); ^{13}C NMR (100 MHz): δ_C 13.5, 21.9, 27.8, 29.2, 30.8, 34.5, 119.3, 128.7, 136.6 ppm; MS: *m*/*z* HRMS/EI: theoretical mass: 388.1023, found mass: 388.1021 Da; ν_{max} ATR-IR/cm^{-1}: 3114, 2954, 2924, 2853, 1500, 1226, 1125, 1032 and 955.

5,7-Dibromo-2,3-bis(methylthio)-[1,4]dithiino[2,3-*c*]furan (9)

Compound **7** (0.100 g, 4.00 mmol) was dissolved in dichloromethane (20 ml) and treated with *N*-bromosuccinimide (0.150 g, 0.841 mmol). This mixture was stirred for 4 h at room temperature then quenched with water (50 ml) and the organic phase was separated. The organic layer was further washed with saturated sodium sulfite solution (50 ml), water (50 ml), before drying

with $MgSO_4$. The solvent was removed under reduced pressure and the crude product was purified by passing through a plug of silica gel with 10% dichloromethane/hexane eluent to afford a brown semi solid (0.146 g, 91%). This was used immediately further without further purification; ^{1}H NMR (400 MHz, $CDCl_3$): δ_H 2.46 (6H, s, $S(CH_3)_2$); ^{13}C NMR (125 MHz): δ_C 18.6, 29.7 (traces of hexane), 117.1, 120.8, 127.5 ppm; MS: *m/z* GC/EI, monoisotopic peak: 404.01 Da.

2,3-Bis(methylthio)-5,7-di(thiophen-2-yl)-[1,4]dithiino[2,3-*c*] furan (11)

Tetrakis(triphenylphosphine) palladium(0), (46 mg, 0.4 μmol, 10% mol) was added to a mixture of compound **9** (150 mg, 4.0 mmol) and 2-(tributylstannyl)thiophene **10** (0.3 ml, 8.9 mmol), dissolved in tetrahydrofuran (20 ml). The reaction mixture was refluxed under N_2 for 24 h. The mixture was then cooled, quenched with water (200 ml) and extracted with dichloromethane (3 × 100 ml). The organic phases were combined and dried over $MgSO_4$ and the solvent removed under reduced pressure. The residue was purified by column chromatography on silica gel, using 20% dichloromethane in hexane as eluent, to give a yellow crystalline solid (37 mg, 22%); ^{1}H NMR (500 MHz, $CDCl_3$): δ_H 2.51 (6H, s, 2 × CH_3), 7.12 (1H, d, ^3J = 3.5 Hz, Ar-H), 7.13 (1H, d, ^3J = 3.5 Hz, Ar-H), 7.36 (2H, dd, ^3J = 5.3 Hz, ^4J = 1.0 Hz, Ar-H), 7.42 (2H, dd, ^3J = 3.8 Hz, ^4J = 1.0 Hz, Ar-H); ^{13}C NMR (100 MHz): δ_C 18.2, 114.8, 123.9, 124.0, 125.2, 128.1, 130.7, 141.3 ppm; MS: *m/z* LDI: 412.0 Da; ν_{max} ATR-IR/cm^{-1}: 3101, 2915, 1466, 1418, 1257, 1080, 1045, 1030 and 989. MS: HRMS/EI: theoretical mass: 411.9212, found mass: 411.9213. Mpt: 97–98 °C.

Acknowledgements

We thank the EPSRC and DSTL for providing a research grant to S.K., Miss Patricia Keating for mass spectrometry and Mrs Denise Gilmour for elemental analysis.

Notes and references

1 A. A. Argun, P.-H. Aubert, B. C. Thompson, I. Schwendeman, C. L. Gaupp, J. Hwang, N. J. Pinto, D. B. Tanner, A. G. MacDiarmid and J. R. Reynolds, *Chem. Mater.*, 2004, **16**, 4401.
2 R. J. Mortimer, A. L. Dyer and J. R. Reynolds, *Displays*, 2006, **27**, 2.
3 O. Hagemann, M. Jorgensen and F. C. Kerbs, *J. Org. Chem.*, 2006, **71**, 5547.
4 G. Dennler, M. C. Scharber and C. J. Brabec, *Adv. Mater.*, 2009, **21**, 1323.
5 J. C. Bernede, *J. Chil. Chem. Soc.*, 2008, **53**, 1549.
6 M. Mas-Torrent and C. Rovira, *Chem. Soc. Rev.*, 2007, 827.
7 S. Allard, M. Forster, B. Souharce, H. Thiem and U. Scherf, *Angew. Chem., Int. Ed.*, 2008, **47**, 4070.
8 F. C. Krebs and H. Spanggaard, *Sol. Energy Mater. Sol. Cells*, 2005, **88**, 363.
9 J. E. Frommer and R. R. Chance, *Encyclopedia of Polymer Science and Engineering*, Wiley, New York, 1986.
10 C. M. Lambert, *Mater. Today*, 2004, **7**, 28.
11 S. K. Deb, *Appl. Opt.*, 1969, (suppl. 3), 193.
12 S. K. Deb, *Sol. Energy Mater. Sol. Cells*, 1995, **39**, 191.
13 Z. Y. Wang, J. Zhang, X. Wu, M. Birau, G. Yu, H. Yu, Y. Qi, P. Desjardins, X. Meng, J. P. Gao, E. Todd, N. Song, Y. Bai, A. M. R. Beaudin and G. LeClair, *Pure Appl. Chem.*, 2004, **76**, 1435.
14 P. M. Beaujuge and J. R. Reynolds, *Chem. Rev.*, 2010, **110**, 268.
15 R. J. Mortimer, *Electrochim. Acta*, 1999, **44**, 2971.
16 L. Groenendaal, F. Jonas, D. Freitag, H. Pielartzik and J. R. Reynolds, *Adv. Mater.*, 2000, **12**, 481.
17 Y. Coskun, A. Cirpan and L. Toppare, *Mater. Sci. Technol.*, 2007, **42**, 368.
18 P. M. S. Monk, R. J. Mortimer and D. R. Rosseinsky, *Electrochromism and Electrochromic Devices* 2007, ch. 1.2, pp. 4–6.
19 R. A. Colley, P. M. Budd, J. R. Owen and S. Balderson, *Polym. Int.*, 2000, **49**, 371.
20 *Handbook of Conducting Polymers*, ed. T. A. Skotheim and J. R. Reynolds, Marcel-Dekker, New York, 2nd edn, 1997.
21 G. Allen, Smart Coatings Markets-2011, Nanomarkets, LC, 2011.
22 R. J. Mortimer, A. L. Dyer and J. R. Reynolds, *Displays*, 2006, **27**, 2.
23 H. Naarmann, *Polymers, Electrically Conducting*, Wiley, 2005.
24 G. Inzelt, *Conducting Polymers: a New Era in Electrochemistry*, Springer, Berlin/Hiedelberg, 2008.
25 L. Groenendaal, G. Zotti, P. H. Aubert, S. M. Waybright and J. R. Reynolds, *Adv. Mater.*, 2003, **15**, 855.
26 C. G. Granqvist, P. C. Lansåker, N. R. Mlyuka, G. A. Niklasson and E. Avendaño, *Sol. Energy. Mater.*, 2009, **19**, 2354.
27 Y. Ding, M. A. Invernale, D. M. D. Mamangun, A. Kumar and G. A. Sotzing, *J. Mater. Chem.*, 2011, **21**, 11873.
28 V. Jain, R. Sahoo, S. P. Mishra, J. Sinha, R. Montazami, H. M. Yochum, J. R. Heflin and A. Kumar, *Macromolecules*, 2009, **42**, 135.
29 J. Roncali, *Chem. Rev.*, 1992, **92**, 711.
30 T. Ito, H. Shirakawa and J. S. Ikeda, *J. Polym. Sci., Polym. Chem. Ed.*, 1974, **12**, 11.
31 R. D. McCullogh, *Adv. Mater.*, 1998, **10**, 93.
32 I. Osaka and R. D. McCullogh, *Acc. Chem. Res.*, 2008, **41**, 1202.
33 S. S. Zade, N. Zamoshchik and M. Bendikov, *Chem.–Eur. J.*, 2009, **34**, 8613.
34 A. Patra and M. Bendikov, *J. Mater. Chem.*, 2010, **20**, 422.
35 M. Heeney, W. Zhang, D. J. Crouch, M. L. Chabinyc, S. Gordeyev, R. Hamilton, S. J Higgins, P. J. Skabara, D. Sparrowe and S. Tierney, *Chem. Commun.*, 2007, 5061.
36 I. Garcia Cuesta, J. Aragó, E. Ortí and P. Lazzeretti, *J. Chem. Theory Comput.*, 2009, **5**, 1767.
37 M. Talu, M. Kabasakaloglu, F. Yildirim and B. Sari, *Appl. Surf. Sci.*, 2001, **181**, 51.
38 U. H. F. Bunz, *Angew. Chem., Int. Ed.*, 2010, **49**, 5037.
39 F. Benvenuti, A. M. R. Galletti, C. Carlini, G. Sbrana, A. Nannini and P. Bruschi, *Polymer*, 1997, **38**, 4973.
40 M. J. González-Tejera, E. Sánchez de la Blanca and I. Carrilo, *Synth. Met.*, 2008, **158**, 165.
41 Y.-S. Lin, C.-Y. Lin, D.-Y. Huang and T. Y. R. Tsai, *J. Chin. Chem. Soc.*, 2005, **52**, 849.
42 C. H. Woo, P. M. Beaujuge, T. W. Holcombe, O. P. Lee and J. M. J. Fréchet, *J. Am. Chem. Soc.*, 2010, **132**, 15547.
43 S. Glenis, M. Benz, E. LeGoff, J. L. Schindler, C. R. Kannewurf and M. G. Kanatzidis, *J. Am. Chem. Soc.*, 1993, **115**, 12519.
44 A. Benahmed-Gasmi, P. Frère and J. Roncali, *J. Electroanal. Chem.*, 1996, **406**, 231.
45 O. Gidron, L. J. W. Shimon, G. Leitus and M. Bendikov, *Org. Lett.*, 2012, **2**, 502.
46 O. Gidron, Y. Diskin-Posner and M. Bendikov, *J. Am. Chem. Soc.*, 2010, **132**, 2148.
47 O. Gidron, A. Dadvand, Y. Sheynin, M. Bendikov and D. F. Perepichka, *Chem. Commun.*, 2011, **47**, 1976.
48 T. Minari, Y. Miyata, M. Terayama, T. Nemoto, T. Nishinaga, K. Komatsu and S. Isoda, *Appl. Phys. Lett.*, 2006, **88**, 083514–083521.
49 A. Hucke and M. P. Cava, *J. Org. Chem.*, 1998, **63**, 7413.
50 R. Berridge, S. P. Wright, P. J. Skabara, A. Dyer, T. Steckler, A. A. Argun, J. R. Reynolds, R. W. Harrington and W. Clegg, *J. Mater. Chem.*, 2007, **17**, 225.
51 J. C. Forgie, A. L. Kanibolotsky, P. J. Skabara, S. J. Coles, M. B. Hursthouse, R. W. Harrington and W. Clegg, *Macromolecules*, 2009, **42**, 2570.
52 R. Akue-Gedu and B. Rigo, *Org. Synth.*, 2005, **82**, 179.
53 N. Svenstrup and J. Becher, *Synthesis*, 1995, **3**, 215.
54 P. Leriche, A. Gorgues, M. Jubault, J. Becher, J. Orduna and J. Garin, *Tetrahedron Lett.*, 1995, **36**, 1275.
55 P. Leriche, S. Roquet, N. Pillerel, G. Mabon and P. Frère, *Tetrahedron Lett.*, 2003, **44**, 1623.
56 J. L. Bredas and G. B. Street, *Acc. Chem. Res.*, 1985, **18**, 309.

57 A. J. Heeger, S. Kivelson, R. J. Serieffer and W.-P. Su, *Rev. Mod. Phys.*, 1988, **60**, 782.
58 H. Münstedt, *Polymer*, 1986, **6**, 899.
59 B. Sun, J. J. Jones, R. P. Burford and M. Skyllas-Kazacos, *J. Mater. Chem.*, 1989, **24**, 4024.
60 Z. T. de Oliveira Jr and M. C. dos Santos, *Solid State Commun.*, 2000, **114**, 49.
61 *CIE* Colorimetry(Official Recommendation of The International Commission on Illumination): CIE Publication no. 15: CIE, Paris, 1971.
62 H. S. Fairman, M. H. Brill and H. Hemmendinger, *Color Res. Appl.*, 1997, **22**, 11.
63 P. M. S. Monk, R. J. Mortimer and D. R. Rosseinsky, *Electrochromism and Electrochromic Devices*, 2007, ch. 4.5, pp. 62–71.
64 B. D. Reeves, C. R. G. Grenier, A. A. Argun, A. Cirpan, T. D. McCarley and J. R. Reynolds, *Macromolecules*, 2004, **37**, 7559.
65 A. W. Bott, *Curr. Sep.*, 2001, **19**, 71.
66 A. W. Bott and W. R. Heineman, *Curr. Sep.*, 2004, **20**, 121.
67 C. L. Guapp, D. M. Welsh, R. D. Rauh and J. R. Reynolds, *Chem. Mater.*, 2002, **14**, 3964.
68 R. W. W. Hooft, *COLLECT*, Nonius BV, Delft, Netherlands, 1998.
69 Z. Otwinowski and W. Minor, Macromolecular Crystallography, Part A, in *Methods in Enzymology*, ed. W. Carter Jr and R. M. Sweet, Academic Press, 1997, vol. 276, pp. 307–326C.
70 G. M. Sheldrick, *Acta Crystallogr., Sect. A: Found. Crystallogr.*, 1990, **46**, 467.
71 O. V. Dolomanov, L. J. Bourhis, R. J. Gildea, J. A. K. Howard and H. Puschmann, *J. Appl. Cryst.*, 2009, **42**, 339.
72 R. Berridge, I. M. Serebryakov, P. J. Skabara, E. Ortí, R. Viruela, R. Pou-Amérigo, S. J. Coles and M. B. Hursthouse, *J. Mater. Chem.*, 2004, **14**, 2822.

